



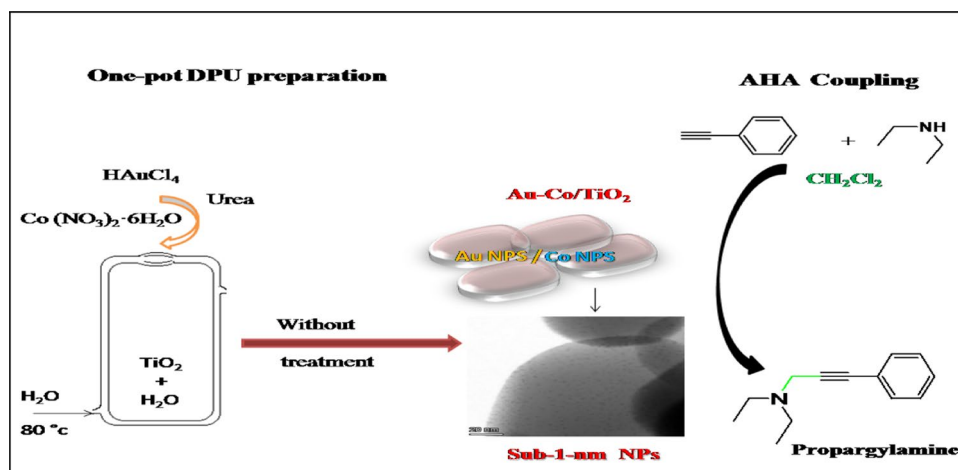
Nano and Sub-nano Gold–Cobalt Particles as Effective Catalysts in the Synthesis of Propargylamines via AHA Coupling

Meriem Bensaad¹ · Amina Berrichi^{1,2} · Redouane Bachir¹ · Sumeya Bedrane¹

Received: 6 July 2020 / Accepted: 30 August 2020 / Published online: 8 September 2020
© Springer Science+Business Media, LLC, part of Springer Nature 2020

Abstract Titania supported Au–Co catalysts with nano- and sub-nanoparticles, were prepared with 1% Au and different contents of cobalt by one pot deposition precipitation with urea. Monometallic gold and cobalt catalysts were also prepared by the same method for a comparative purpose. The characterization of bimetallic catalyst evidenced the presence of sub-nanoparticles where 50% of cobalt and 40% of gold particles are smaller than 1 nm and the formation Au–Co particles. The results show a positive effect of cobalt on gold particles size and the catalytic activity. The effectiveness of these catalysts in the synthesis of several propargylamines via amine, CH_2Cl_2 and alkyne coupling (AHA coupling) was demonstrated. Different propargylamines were synthesized with very good yields (71%–88%). A comparative study of monometallic gold, monometallic cobalt and bimetallic gold–cobalt catalysts was investigated. The most efficient catalyst was reused for up to six reaction cycles without significant activity loss.

Graphic Abstract



Keywords Sub-nano · Gold nanoparticles · Bimetallic nanoparticles · Propargylamine · AHA coupling

1 Introduction

Gold has attracted many researchers because since its surprising catalytic activity was evidenced in CO oxidation [1]. However, gold catalytic activity depends widely on the particles size, with an optimum when gold particles are in the range of 1–5 nm [2]. The gold catalyst synthesis is consequently a key step to afford nanoparticles smaller than 5 nm

✉ Amina Berrichi
berrichi.amina@yahoo.fr

¹ Laboratory of Catalysis and Synthesis in Organic Chemistry, University of Tlemcen, BP 119, Tlemcen, Algeria

² Sciences Institut, University Center Belhadj Bouchaib, BP 284, 46000 Ain Témouchent, Algeria

[3], because of their activity and stability, mono-dispersed gold NPs were described in the literature, sub-10, sub-5, and sub-2 nm synthesized with several methods [4].

Several methods have been investigated for gold sub-nanoparticles preparation, and it is still difficult because of the lack of reproducibility despite a high level of control and specific reagents. The combination of gold with different metals such as copper [5], silver [6], palladium [7], Nickel [8], iron [9] and cobalt is an interesting way. Gold based bimetallic systems are known to exhibit higher catalytic activity in different reactions such as the water–gas shift reaction [10], Oxidation [11], hydrogenation [12], hydrogen production and amidation reactions [13, 14].

Supported Au–Co catalysts have a high activity due to synergetic effect between Au NPs and cobalt species. The preparation method is the key parameter of NPs formation. Gamboa and colleagues [15] prepared Au–Co/CeO₂ catalyst by metals successive deposition on the support. In fact, the cobalt catalyst was prepared by incipient wetness impregnation (IWI) while gold was introduced by a deposition precipitation method (DP). The authors showed the Co₃O₄ particles with size ranging from 11 to 19 nm. The same catalyst was prepared by deposition precipitation method (DP) [16]; sub-5 nanoparticles were obtained.

Electroless metal deposition [17] was also used, where the Au(Co)/Ti catalysts were prepared following two-steps: electroless cobalt deposition and gold displacement from the tetrachloro-complex solution. The preparation led to Au nanoparticles crystallites with a cubic shape and size ranging from 30 to 100 nm. Then, Au–Co(III)/SAC [18] was prepared by the incipient wetness impregnation where Au nanoparticles have an average size of 4 nm. The authors showed that the addition of Co result a slight increase of the particles size. In 2014, Xu and colleagues [11] prepared Au–Co/SiO₂ with an average size of 2.5 nm. They prepared firstly the Au/SiO₂ by impregnation, later, the cobalt was deposited on the parent catalyst. Supported bimetallic Au–Co/SBA-1 was also prepared by impregnation and deposition–precipitation with urea (DPU) [19]. The characterization showed the presence of gold particles and cobalt oxide Co₃O₄. The DPU method usually used for the synthesis of mono sub-5 nm Au NPs on oxides [3].

Barrios and colleagues [13] used the consecutive steps incipient wetness impregnation to modify TiO₂ by three different metals (Ni, Co and Pd) and gold was deposited by the DP method. All samples have an average particles size in the range of 3–4 nm. Finally, in Santos's study [20], the catalyst was prepared by a three-step process, anodization of titanium (Ti), electroless cobalt deposition and a spontaneous Au displacement from the Au-containing solution. All preparation methods of gold–cobalt catalysts included two or three steps leading to Au NPs larger than 2 nm.

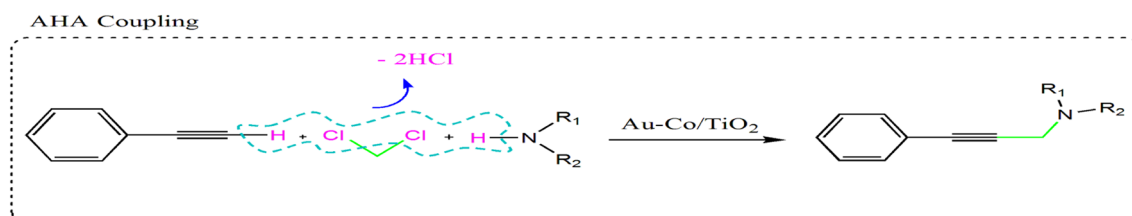
Furthermore, propargylamines are key intermediate for the synthesis of several chemicals [21, 22], and biologically active molecules such as inhibitors of Parkinson's disease [23–25]. Different propargylamines were synthesized through the one-pot three-component coupling reactions of amines, alkynes and aldehydes (A3 coupling) using homogenous gold [26–30], cobalt [31] and others catalysts [32].

Heterogeneous monometallic gold [33–50] and cobalt catalysts [51] were also used for this coupling.

Recently, haloalkanes were used as a source of methylene fragment for the propargylamines synthesis. The coupling of amines, haloalkane and alkynes (AHA coupling) remains limited compared to A3 coupling [52–54] particularly under heterogeneous conditions, where very few catalysts are reported, such as Au/CeO₂ [55] or SiO₂/APTES/DAFO–Fe [56] and recently Au–Co/CeO₂ [57].

The main objective of this work is the preparation of a supported catalyst containing nano and sub-nanoparticles, ideally smaller than 1 nm. The trick is the cobalt use to increase gold dispersion and obtain gold and cobalt sub-nanoparticles.

The catalyst was prepared by one pot-DPU method (one pot deposition precipitation by urea) in a parallel ways and under the same conditions of pH and it used for amines, haloalkane and alkyne coupling (AHA coupling) to synthesize propargylamines (Scheme 1).



Scheme 1 Synthesis of propargylamines via AHA coupling

2 Experimental

2.1 Reagents and Characterization Methods

$\text{HAuCl}_4 \cdot 3\text{H}_2\text{O}$, $\text{Co}(\text{NO}_3)_2 \cdot 6\text{H}_2\text{O}$, TiO_2 powder, amines, and phenylacetylene were purchased from Sigma–Aldrich and used directly as the main starting materials without further purification.

Atomic absorption spectroscopy analysis (AAS) was carried out with a Perkin Elmer Instrument Analyst 300 with flame.

Powder X-rays diffraction (XRD) patterns were collected using an Ultima III Rigaku Monochromatic Diffractometer using $\text{Cu K}\alpha$ radiation ($\lambda = 1.5406 \text{ \AA}$). Angle powder XRD were obtained at the same scanning rate of $1/\text{min}$ in the 2θ range $20\text{--}80^\circ$.

Diffuse reflectance spectroscopy (DR-UV-Vis) measurements were carried at room temperature with Lambda 800 UV/Vis spectrometer in the range of $200\text{--}800 \text{ nm}$.

Transmission Electron Microscopy (TEM) was carried out on a JEM-1230 electron microscope (JEOL, Tokyo) with an acceleration voltage of 80 kV . All samples were dispersed in ethanol and sonicated for 20 min .

2.2 Catalyst Preparation

Monometallic catalysts $1\% \text{ Au/TiO}_2$ and $x\% \text{ Co/TiO}_2$ were prepared by DPU (Deposition–Precipitation with Urea). This method is described elsewhere [9, 57].

The bimetallic gold–cobalt catalysts $1\% \text{ Au-x}\% \text{ Co/TiO}_2$ with different cobalt loadings were prepared by one pot deposition precipitation with urea (one-pot DPU). For $1\% \text{ Au-1}\% \text{ Co/TiO}_2$, a suspension of 2 g of TiO_2 in 200 mL of distilled water was introduced into a double walls glass reactor. The suspension was heated at 80°C , then 4 mL of $\text{HAuCl}_4 \cdot 3\text{H}_2\text{O}$ (aqueous solution at 10 g/L), 62.4 mL of $\text{Co}(\text{NO}_3)_2 \cdot 6\text{H}_2\text{O}$ (aqueous solution at 10 g/L) and 900 mg of urea were added in the same time (one pot) under vigorous stirring. The suspension was stirred at 80°C for 16 h in the absence of light. The solid obtained was separated by centrifugation, washed several times with distilled water and dried at 80°C overnight.

2.3 Synthesis of Propargylamines via AHA Coupling

In this study, the propargylamine was synthesized via the activation of the C–Cl bond of CH_2Cl_2 and the terminal alkynes C–H bond.

A terminal alkyne (2 mmol), amine (2.2 mmol), CH_2Cl_2 (3 mL), DABCO (2 mmol), and catalyst (80 mg) were

mixed with solvent (3 mL) under N_2 at 65°C . After 24 h , the reaction mixture was diluted with CH_2Cl_2 and the catalyst was recovered by centrifugation.

The mixture was extracted with water/ CH_2Cl_2 and dried over Na_2SO_4 . Evaporation of the solvent furnished the crude product which was purified by column chromatography. The reaction products were known compounds and confirmed by NMR, GC–MS and FTIR spectroscopy.

1,4-Diphenylbuta-1,3-diyne

$^1\text{H NMR}$ (400 MHz , CDCl_3) (δ ppm): $7.42\text{--}7.44$ (m, 4H), $7.24\text{--}7.27$ (m, 6H);

$^{13}\text{C NMR}$ (100 MHz , CDCl_3) (δ ppm): 132.6 , 129.3 , 128.5 , 122.1 , 81.8 , 75.2 ;

MS (EI) m/z : 202 , 174 , 126 , 101 , 88 .

N,N-Diethyl-3-phenylprop-2-yn-1-amine

$^1\text{H NMR}$ (400 MHz , CDCl_3) (δ ppm): $1.10\text{--}1.136$ (t, 6H, 2CH_3), $2.60\text{--}2.66$ (q, 4H, 2CH_2), 3.643 (s, 2H, CH_2), $7.27\text{--}7.30$ (m, 3Har), $7.41\text{--}7.43$ (m, 2Har);

$^{13}\text{C NMR}$ (100 MHz , CDCl_3) (δ ppm): 11.61 , 40.44 , 46.31 , 83.34 , 83.96 , 122.35 , 126.89 , 127.20 , 130.69 ;

MS: $m/z = 188.089$, 115.027 ($-\text{HN}(\text{CH}_2\text{CH}_3)_2$).

IR (ν , cm^{-1}) = 760 , 689 , 1198 , 1320 ;

The results presented in this article are propargylamines yields, TON_{Au} and TON_{tot} .

TON_{Au} is calculated by considering that Au is the sole to have a catalytic activity while the TON_{tot} is calculated by considering that Au and Co are both active.

$\text{TON}_{\text{Au}} = \text{moles of product formed/moles of Au atoms exposed on the catalyst surface}$.

TON_{tot} is calculated by considering that Au and Co are both active.

$\text{TON}_{\text{tot}} = \text{moles of product formed/moles of (Au + cobalt) atoms exposed on the catalyst surface}$.

$\text{Yield (\%)} = 100 \times \frac{\text{experimental weight of propargylamine}}{\text{theoretical weight of propargylamine}}$.

3 Results and Discussion

3.1 Catalysts Characterization

Metal loadings of Au and Co for $1\% \text{ Au/TiO}_2$ and different $1\% \text{ Au-x}\% \text{ Co/TiO}_2$ catalysts were measured by atomic absorption spectroscopy (AAS) in order to check the efficiency of Co-DPU method to deposit both gold and cobalt on TiO_2 in the same time. Results reported in Table 1 show a good agreement between the amount of gold theoretically introduced ($1\% \text{ Au}$) and that actually deposited.

For low percentages ($1\% \text{ Co}$ and $2\% \text{ Co}$) the experimental values of deposited cobalt are very close to the theoretical values. However, with a high Co content (4% and 6%), the amounts actually deposited are lower than

Table 1 Gold and cobalt loadings as measured by atomic absorption spectroscopy (AAS)

Catalyst	Au (wt%) ^a	Au (wt%) ^b	Co (wt%) ^a	Co (wt%) ^b
Au/TiO ₂	1	0.80	0	0
Co/TiO ₂	0	0	1	0.80
Au–Co/TiO ₂ (1)	1	0.86	1	0.80
Au–Co/TiO ₂ (2)	1	0.99	2	2
Au–Co/TiO ₂ (3)	1	0.89	4	2.64
Au–Co/TiO ₂ (4)	1	0.71	6	3

^aTheoretical content

^bExperimental content

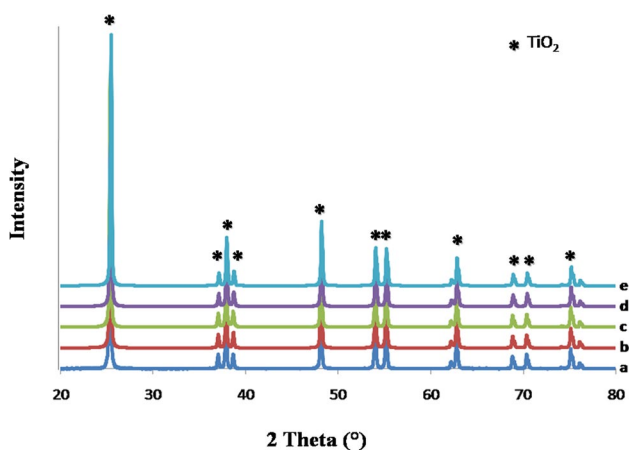


Fig.1 XRD patterns of (a) TiO₂, (b) 1%Co/TiO₂, (c) 1%Au/TiO₂, (d) Au–Co/TiO₂ (1) and (e) Au–Co/TiO₂(4) 254×190 mm (96×96 DPI)

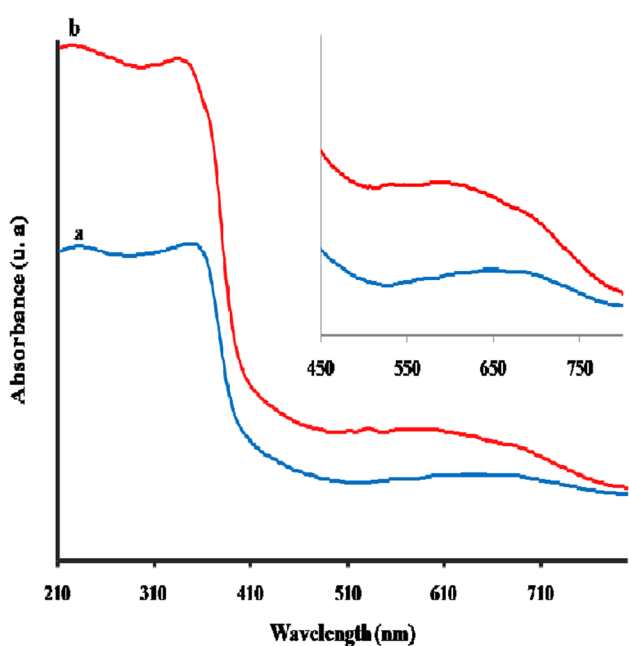


Fig.2 Diffuse-reflectance UV–visible spectra of **a** Au/TiO₂ and **b** Au–Co/TiO₂ (4) 346×169 mm (120×120 DPI)

those theoretically expected. This is probably related to the saturation of the support surface at such a high metal load.

These results indicate that the Co–DPU method is very efficient for the deposition up to 1% Au and 2% Co, however for high Co contents; the amounts actually deposited are generally lower than those expected.

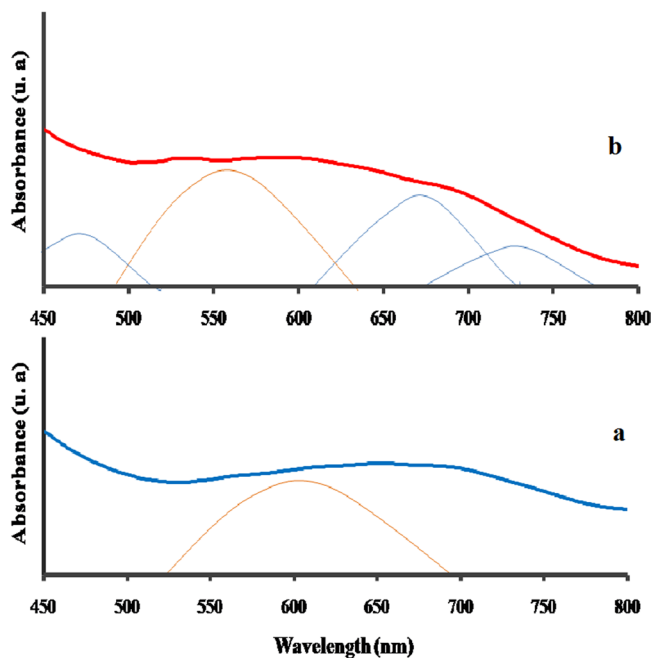
To evidence the nature of cobalt species, samples were characterized by XRD. The bimetallic catalysts are compared to the monometallic one in Fig. 1. All samples have peaks at 2θ values of 25.31°, 37.40°, 37.76°, 37.9°, 48.03°, 53.93°, 55.11°, 62.59°, 62.62°, 68.88°, 70.25°, 75.10° and 76,22° which correspond to the TiO₂ diffractions planes (101), (103), (004), (112), (200), (105), (211), (213), (204), (116), (220), (215) and (301) respectively [58].

However, no gold or cobalt diffraction peaks were observed in the monometallic and the bimetallic diffractograms.

This finding indicates that metal particles are smaller than the XRD detection limit. This shows that both gold and cobalt particles are well dispersed on the surface of the support. Unfortunately, this does not inform about the crystallographic structures of Au and Co or about the interaction between them.

Thus, Au/TiO₂ and Au–Co/TiO₂ were characterized by DR–UV–Vis spectroscopy.

The deconvoluted spectrum of Au/TiO₂ (Fig. 2a) shows a band with a maximum at 600 nm characteristic of the reduced gold nanoparticles plasmon resonance [55].



This band is still visible on the Au–Co/TiO₂ spectrum (Fig. 2b), thus showing the existence of nanoparticles in this catalyst. However, the maximum of this band has shifted towards the lowest values (560 nm) which could be explained by the modification of gold particles environment probably due to interactions with Co [57] indicating the possible formation of bimetallic Au–Co nanoparticles. Nevertheless, the deconvolution of this spectrum reveals characteristic bands of cobalt oxides at 460 nm for Co³⁺ and 670 nm, 730 nm for Co²⁺.

These findings suggest the existence of Au–Co bimetallic nano alloy but also of separated Co particles. However, results are insufficient to decide on the nature of the Au–Co interactions.

In order to rate particles sizes and examine the nature of Au–Co interactions, various electron microscopy techniques were used.

First, Au/TiO₂ and bimetallic Au–Co/TiO₂ (4) were characterized by Transmission Electron Microscopy. The results are shown in Fig. 3 and Fig. 4 respectively.

Figure 3a reveals a homogeneous distribution of gold nanoparticles on TiO₂ surface. The histogram of the particles size distribution (Fig. 3b) indicates that gold nanoparticle sizes range from 2 to 5 nm.

TEM images of the Au–Co/TiO₂ catalyst show a homogeneous distribution of Au and Co particles on the TiO₂ surface (Fig. 4 a).

To assess the particle sizes of gold and Co separately, the Avizo software was used.

The histograms of the particles size distribution for Au (Fig. 4b) and Co (Fig. 4c) indicate that Au particle sizes range from 0.2 to 4 nm and. Co particle sizes range from 0.1 to 5 nm.

These results highlight the presence of sub-nano particles of Au and Co. Indeed, 40% of gold particles and 50% of cobalt particles are in the sub-nano range (smaller than 1 nm).

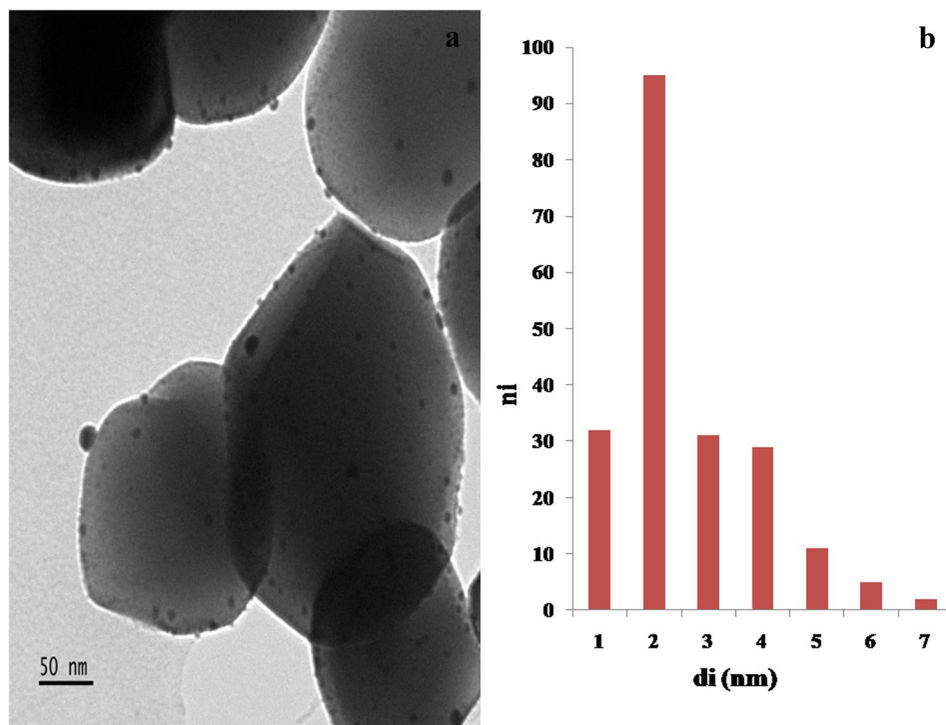
This shows deposition and stabilization of sub-nanoparticles of Au and Co on TiO₂ can be achieved using Co-DPU method.

In order to confirm the hypothesis of the formation of bimetallic Au–Co sub-nanoparticles and nanoparticles suggested earlier following the results of the DR-UV-Vis characterization, Au–Co/TiO₂ catalysts were characterized by (HAADF)-STEM microscopy.

Indeed, scanning/transmission electron microscopy (STEM) using high-angle annular dark field (HAADF)-STEM is one of the most important techniques used to characterize the bimetallic nanoparticles where images with Z-contrast and high-resolution can be acquired.

Figure 5 shows HAADF-STEM images of the Au–Co/TiO₂ catalyst. The figure displays the elemental mapping images for the bimetallic nanoparticle. The blue and red color images are associated with the Co and Au elements, respectively. Also the overlap image is shown. It can be observed that Co (Fig. 5b) and Au (Fig. 5c) are nano and sub-nano sized and have an almost homogeneous distribution on the support surface. The overlap image Fig. 5a

Fig.3 TEM micrograph of **a** Au/TiO₂ and **b** gold particles size plot 254×190 mm (96×96 DPI)



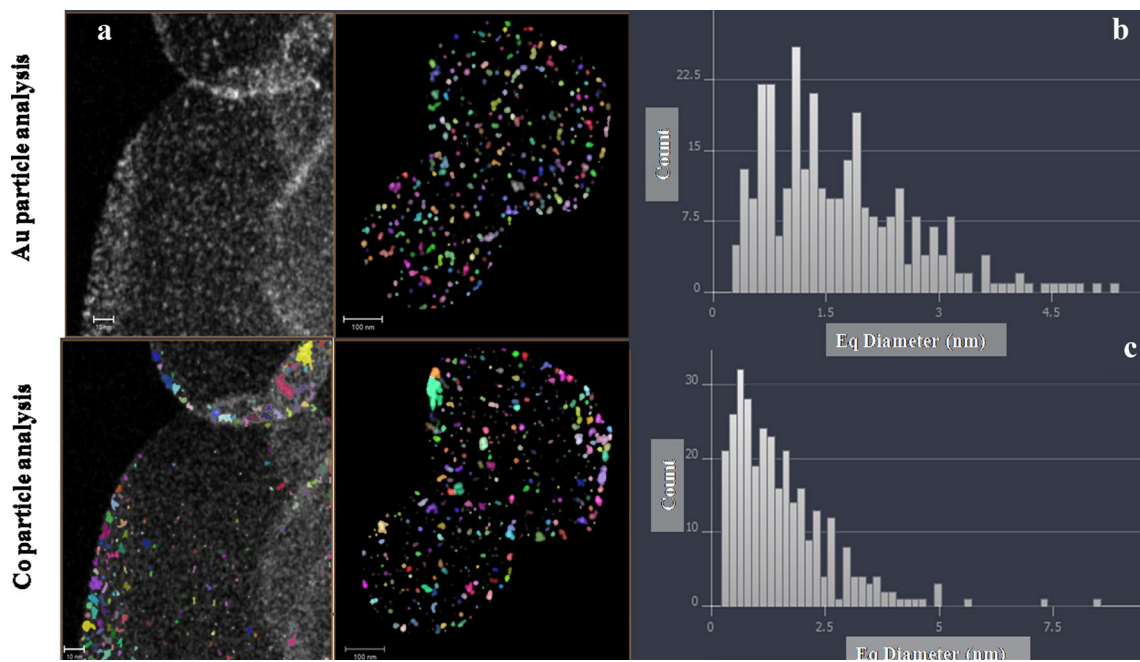


Fig.4 HAADF STEM micrographs of Au–Co/TiO₂ (4), gold and cobalt particles size plot 270 × 151 mm (120 × 120 DPI)

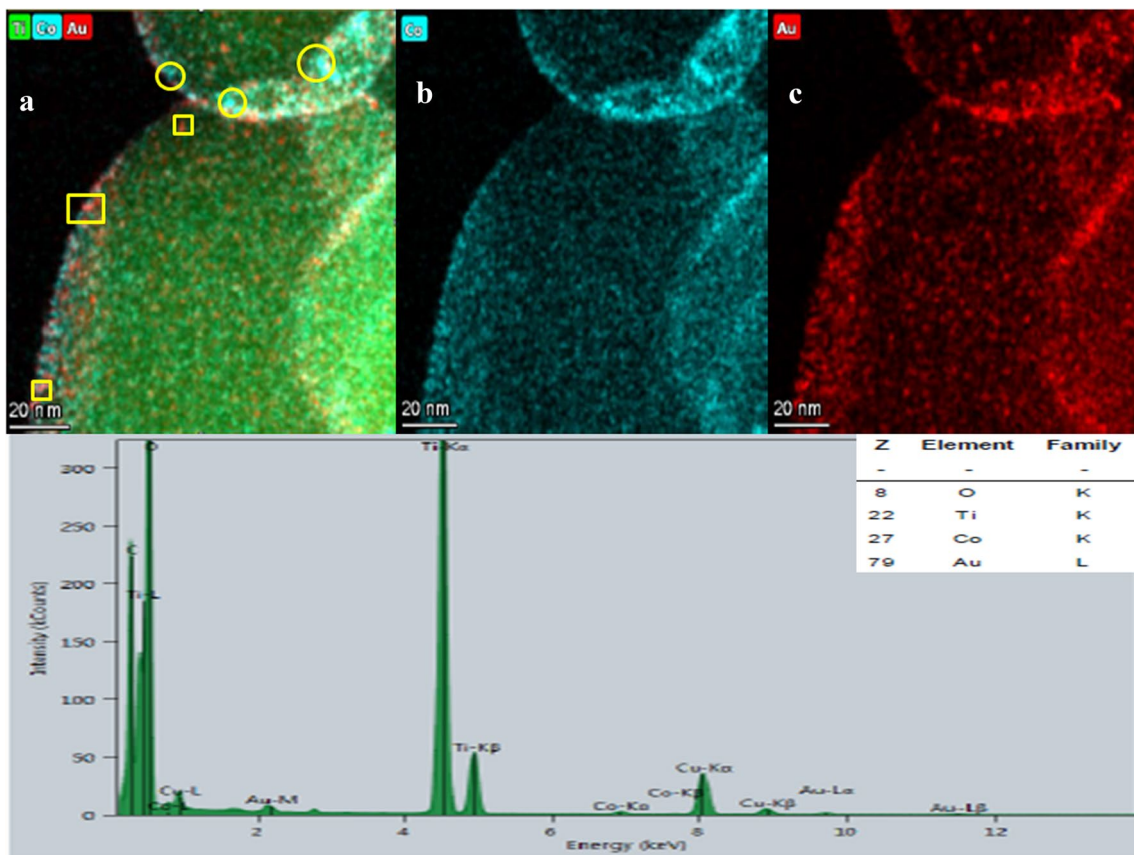


Fig.5 HAADF STEM image of Au–Co/TiO₂ (4), a EDS overlap mapping of Au and Co, EDS mapping of b Co, c Au and EDS analysis 254 × 190 mm (96 × 96 DPI)

shows some zones where cobalt is segregated (circles) but also areas where gold and cobalt overlap (squares). These results clearly show the formation of bimetallic Au–Co particles but also the segregation of some Co particles. To better understand the Au–Co interaction, zooms on

the areas where Au and Co overlap were made. It can be observed on Fig. 6 that the sub nano and nanoparticles have an alloy structure, where Au and Co atoms are localized in the particles in random form.

Fig. 6 HAADF-STEM image of Au–Co alloy bimetallic nano and sub-nanoparticles with EDS mapping of Au, Co and overlap elements for different zones 254 × 190 mm (96 × 96 DPI)

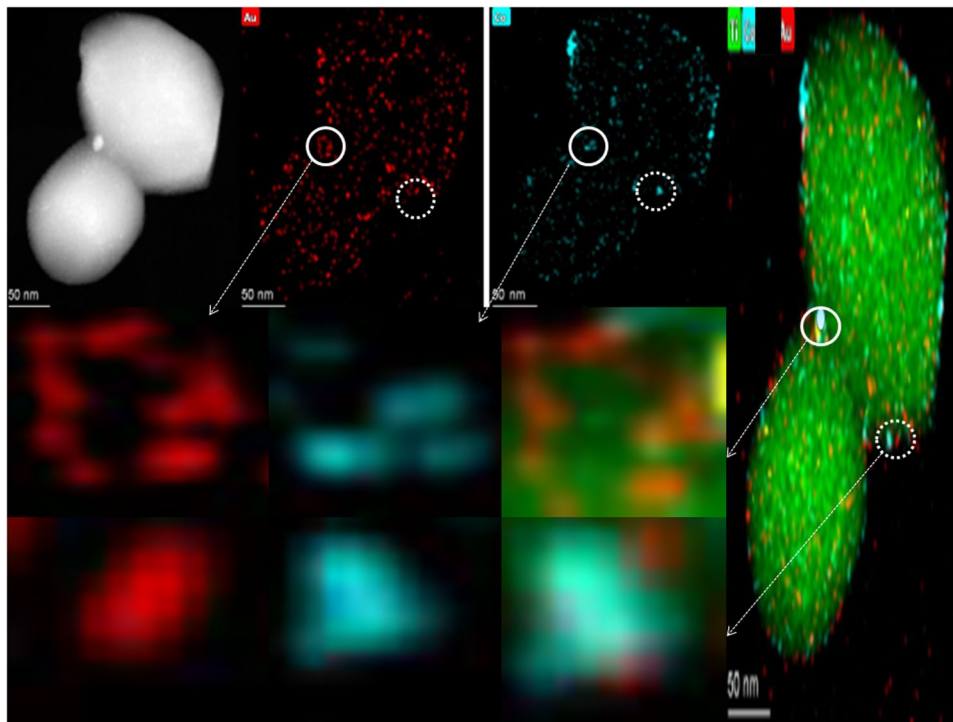
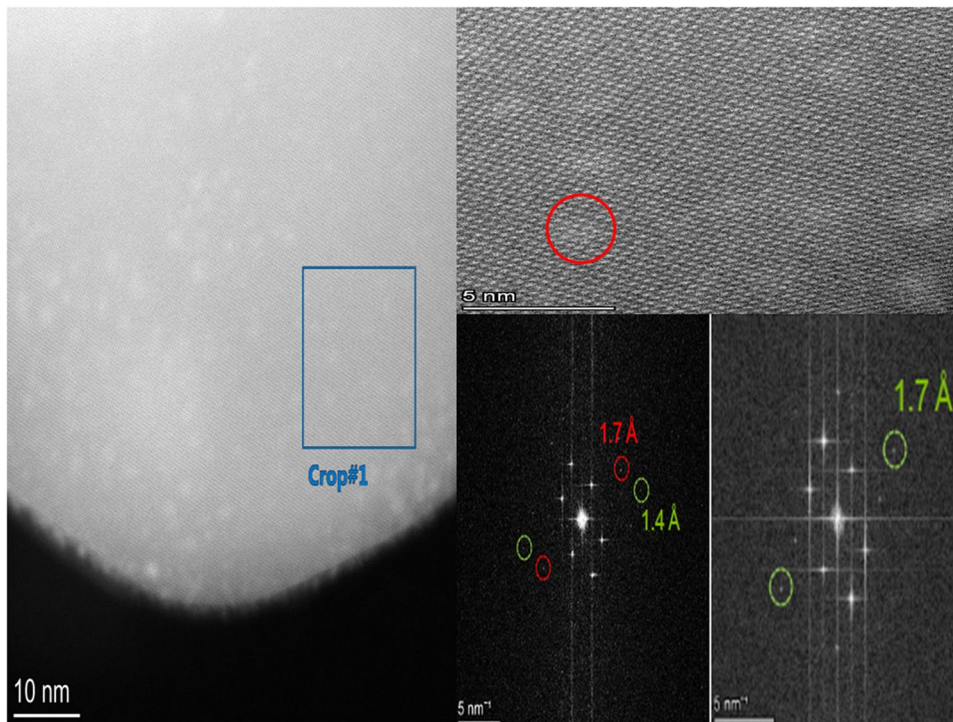


Fig. 7 Drift Corrected Frame Integration (DCF) combined with HR-STEM of the bimetallic Au–Co/TiO₂ (4) catalyst 254 × 190 mm (96 × 96 DPI)



To confirm the above obtained results, HR-STEM combined with Drift Corrected Frame Integration (DCFI) was made. d-spacings of 0.14 nm and 0.17 nm were obtained from Fig. 7. Such d-spacings do not perfectly match with any reflection plane distances of pure Au or Co suggesting that an alloyed Au–Co structure was formed in the particles [59]. Therefore, this confirms the alloy structure of the bimetallic sub nanoparticles and nanoparticles.

3.2 Synthesis of Propargylamines

First, propargylamine (N,N-Diethyl-3-phenyl-prop-2-yn-1-amine) was synthesized via AHA coupling of diethylamine, CH_2Cl_2 and phenylacetylene (Scheme 1) using the monometallic catalysts Au/TiO₂ and Co/TiO₂. Results are summarized in Table 2.

With Au/TiO₂ and Co/TiO₂ catalysts yields of 26% (entry 1) and 16% (entry 2) respectively were obtained. The reaction was subsequently carried out using the bimetallic 1%Au–1%Co/TiO₂ catalyst. An interesting yield of 53% was obtained (entry 3).

This improvement in yield could be attributed either to the summation of Au and Co activities or to an increase in the Au activity when it alloys with Co in the form of Au–Co subnano and nano particles.

In order to verify either of these two hypotheses, the TON of the reaction was calculated according to two ways. The first considers the Au and Co particles both to be Active Sites (TON_{tot}) which means that the TON_{tot} of the Au–Co/TiO₂ catalysts would be comparable to the sum of the two monometallic catalysts TONs. The second considers that Au particles are active sites but Co particles are not (TON_{Au}) which would mean that the TON_{Au} increases when the reaction yield increases although the Au content always remains equal to 1% in all the catalysts.

The results shown in the Table 2 clearly indicate that the TON_{tot} of the 1%Au1%Co/TiO₂ (entry 3) catalyst is

Table 2 Activity of mono and bimetallic catalysts in AHA coupling reaction

Entry	Catalysts	Yield (%)	TON _{Au} ^a	TON _{tot} ^b
1	Au/TiO ₂	26	80	80
2	Co/TiO ₂	16	0	15
3	Au–Co/TiO ₂ (1)	53	152	37
4	Au–Co/TiO ₂ (2)	64	160	20
5	Au–Co /TiO ₂ (3)	70	194	18
6	Au–Co /TiO ₂ (4)	80	286	17

Reaction conditions: Phenylacetylene (2 mmol), diethylamine (2.2 mmol), CH_2Cl_2 (3 mL), DABCO (2 mmol), catalyst (80 mg) and CH_3CN (3 mL), N₂, 24 h, 65 °C

^aTON calculated with Au as the only active site

^bTON calculated with (Au + Co) as active sites

absolutely not equal to the sum of the two monometallic catalysts TONs, even worse it is lower than that of the 1%Au/TiO₂ monometallic catalyst.

However, the TON_{Au} of the bimetallic catalyst is almost twice that of the 1%Au/TiO₂ monometallic catalyst.

In order to verify the effect of Co on Au activity, different catalysts were prepared by keeping gold loading equal to nearly 1wt-% and increasing the cobalt loading from 1 to 3%.

Results in Table 2 show that yields increase when the Co contents increases and reaches up to 80% (entries 3–6). Furthermore, these results confirm the TON_{Au} increases with yields while the TON_{tot} decreases.

For comparison, different monometallic Co/TiO₂ catalysts having the same Co contents as their bimetallic counterpart were prepared and tested. The results shown in the Fig. 8 indicate that cobalt has very little activity and the yield does not exceed 18% whatever the Co content.

These observations reasonably suggest that the active sites in the bimetallic catalyst are the alloyed Au–Co subnano and nano particles. Thus, Co would not be active in itself, but it improves the activity of Au by decreasing the particles size, their stabilization in the form of sub-nanoparticles and by modifying their electron density.

3.3 Synthesis of Different Propargylamines

When this study started, phenylacetylene, dichloromethane and diethylamine were used as initial substrates to synthesize propargylamine and to compare activities of monometallic and bimetallic catalysts.

This study showed that Au–Co/TiO₂ (4) was the best catalyst reaching a propargylamine yield of 80%. This catalyst was therefore selected to synthesize different propargylamines, under similar reaction conditions, and using secondary amines. Very good yields of 77%–88% were obtained (Table 3). The acyclic secondary amines such as dibutylamine and diethylamine gave the same yield (80%). The cyclic secondary amines such as morpholine gave also a good yield (88%). We also checked the activity of sterically secondary amine which worked smoothly to give targeted propargylamines with appreciable yields (Table 3, entry 6).

The catalyst was also successfully used in A3 formaldehyde, morpholine and phenylacetylene coupling using Huang's reaction conditions [37] leading to 71% of product (Table 3, entry 3).

One of the most important criteria in heterogeneous catalysis is the resistance to deactivation. Consequently, the reusability of Au–Co/TiO₂ (4) catalyst was evaluated in the propargylamine synthesis by phenylacetylene, CH_2Cl_2 and diethylamine coupling under the same reaction conditions.

In addition, the reusability of Au–Co/TiO₂ (4) catalyst was compared with that of the monometallic catalyst Au/TiO₂. After the reaction, the catalysts were centrifuged,

Fig.8 Monometallic and bimetallic catalysts activity in AHA coupling 254 × 190 mm (96 × 96 DPI)

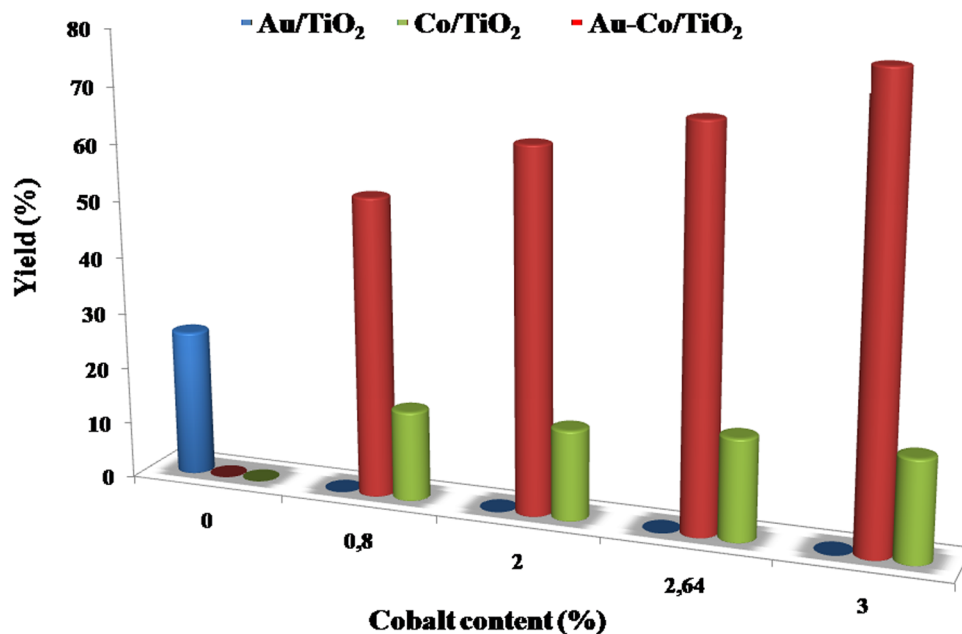


Table 3 Different propargylamines synthesized by AHA and A3 coupling reactions over Au–Co/TiO₂ (4)

Entry	Propargylamine	Yield (%)
1		80
2		88
3		71 ^a
4		77
5		80
6		70

Reaction conditions: Phenylacetylene (2 mmol), Amine (2.2 mmol), CH₂Cl₂ (3 mL), DABCO (2 mmol), catalyst (80 mg) and CH₃CN (3 mL), N₂, 24 h, 65 °C

^aA3 coupling catalyzed by Au–Co/TiO₂ (4) (80 mg)

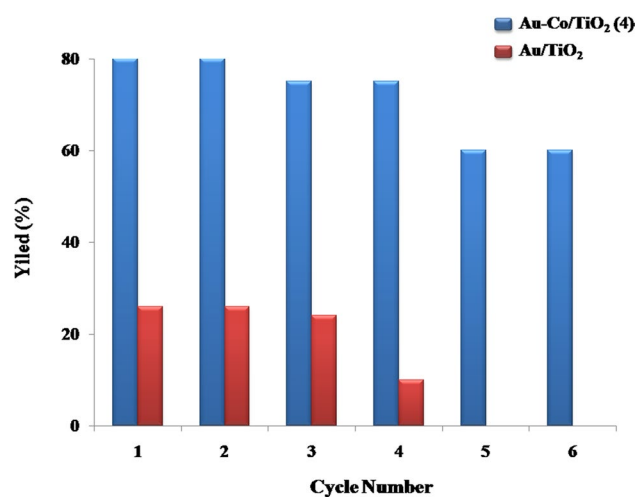
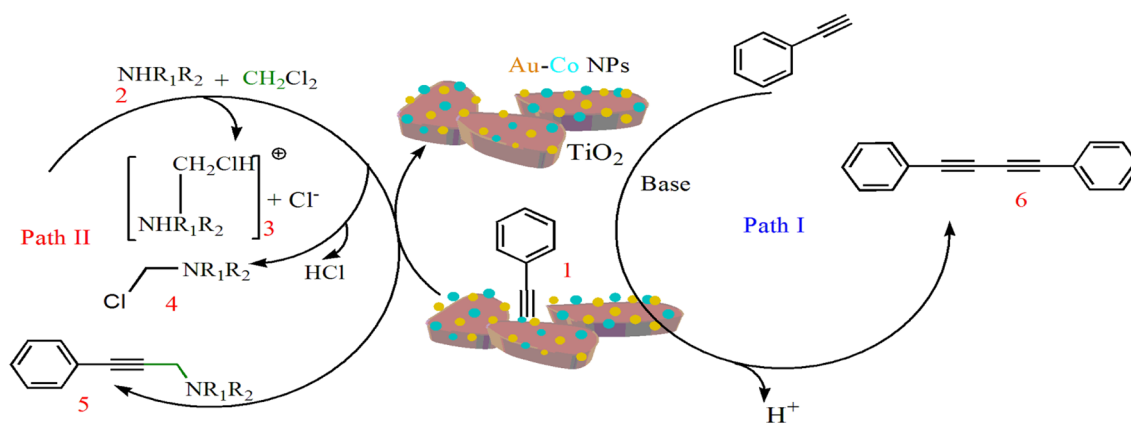


Fig.9 Reusability of Au/TiO₂ and Au–Co/TiO₂ (4) in AHA coupling 254 × 190 mm (96 × 96 DPI)

washed with acetone and dried at 80 °C. Figure 9 shows that the bimetallic catalyst is almost stable and reusable upon six reaction cycles while the reusability of the monometallic decreased after the third cycle. These results show that cobalt stabilized gold sub-nano and nanoparticles and improve their activity. This further confirms a beneficial effect of Co on Au. Finally, according to our earlier and others studies [55, 60–63], the catalytic mechanism for the AHA three-component coupling reaction with CH₂Cl₂, phenylacetylene, and amine is proposed in Scheme 2.

In the absence of CH₂Cl₂, the homocoupling product 6 can be afforded following Path I: the C–H band of phenylacetylene activated by gold–cobalt nanoparticles with



Scheme 2 Proposed AHA reaction mechanism using gold cobalt bimetallic catalyst

generation of the Au–Co acetylide intermediate 1. With CH_2Cl_2 , the propargylamine is formed via AHA coupling following Path II. The reaction of CH_2Cl_2 and amine gives a chloro- $\text{N,N-R}_1\text{R}_2$ -methanaminium chloride salt 3. This compound produces chloro- $\text{N,N-R}_1\text{R}_2$ -methanamine 4 by elimination of HCl . Finally, chloro- $\text{N,N-R}_1\text{R}_2$ -methanamine reacts with an adsorbed molecule of phenylacetylene 1 on the catalyst surface to give the corresponding propargylamine 5.

4 Conclusion

The one pot DPU (one pot deposition precipitation with urea) method has been used successfully to deposit sub-nano and nano particles of Au and Co on TiO_2 .

Different characterization methods have revealed the formation of Au–Co alloys with sub nano and nanometric sizes.

As prepared materials were used efficiently as catalysts for a one pot synthesis of propargylamines via AHA coupling of secondary amines, CH_2Cl_2 and phenylacetylene.

Bimetallic catalysts have been shown to be much more active than parent monometallic catalysts. A TON 4.5 times greater than that of the parent monometallic catalyst was achieved. Thus, various propargylamines were synthesized with very good yields (70%–88%).

This excellent activity of bimetallic catalysts is attributed to the improvement of the activity of Au by Co due to the formation of sub nano and nano bimetallic Au–Co particles.

Finally, the bimetallic catalysts turned out to be very stable since they were reused up to six reaction cycles without significant activity loss.

Acknowledgements This work was funded by the Algerian DGRSDT-MESRS, and the University of Tlemcen. The authors thank the company Thermo Fisher Scientific (Europe NanoPort-Eindhoven-Netherlands) and the company Sinal Algeria for their help in carrying out electron microscopy characterizations.

Compliance with Ethical Standards

Conflict of interest The authors declare that they have no conflicts of interest.

References

- Zhuang Z, Sheng W, Yan Y (2014) Synthesis of monodisperse Au@ Co_3O_4 core-shell nanocrystals and their enhanced catalytic activity for oxygen evolution reaction. *Adv Mater* 26(23):3950–3955
- Hutchings GJ (2005) Catalysis by gold. *Catal Today* 100(1):55–61
- Zanella R, Delannoy L, Louis C (2005) Mechanism of deposition of gold precursors onto TiO_2 during the preparation by cation adsorption and deposition–precipitation with NaOH and urea. *Appl Catal A* 291(1–2):62–72
- Piella J, Bastús NG, Puentes V (2016) Size-controlled synthesis of sub-10-nanometer citrate-stabilized gold nanoparticles and related optical properties. *Chem Mater* 28(4):1066–1075
- Liu X, Wang A, Li L et al (2011) Structural changes of Au–Cu bimetallic catalysts in CO oxidation: in situ XRD, EPR, XANES, and FT-IR characterizations. *J Catal* 278(2):288–296
- Kowalska E, Janczarek M, Rosa L et al (2014) Mono- and bimetallic plasmonic photocatalysts for degradation of organic compounds under UV and visible light irradiation. *Catal Today* 230:131–137
- Cybula A, Priebe JB, Pohl MM et al (2014) The effect of calcination temperature on structure and photocatalytic properties of Au/Pd nanoparticles supported on TiO_2 . *Appl Catal B* 152–153(1):202–211
- Suo Z, Lv A, Lv H et al (2009) Influence of Au promoter on hydrodesulfurization activity of thiophene over sulfided Au–Ni/SiO₂ bimetallic catalysts. *Catal Commun* 10(8):1174–1177
- Ameur N, Berrichi A, Bedrane S et al (2014) Preparation and characterization of Au/Al₂O₃ and Au–Fe/Al₂O₃ materials, active and selective catalysts in oxidation of cyclohexene. *Adv Mater Res* 856:48–52
- Wu S-K, Lin R-J, Jang S et al (2013) Theoretical investigation of the mechanism of the water-gas shift reaction on cobalt@ gold core-shell nanocluster. *J Phys Chem* 118(1):298–309
- Xu X, Fu Q, Wei M et al (2014) Comparative studies of redox behaviors of Pt–Co/SiO₂ and Au–Co/SiO₂ catalysts and their activities in CO oxidation. *Catal Sci Technol* 4(9):3151–3158

12. Díaz G, Gómez-Cortés A, Hernández-Cristobal O et al (2011) Hydrogenation of citral over Ir–Au/TiO₂ catalysts. Effect of the preparation method. *Top Catal.* 54:467–473
13. Barrios C, Albiter E, Jimenez JG et al (2016) Photocatalytic hydrogen production over titania modified by gold–Metal (palladium, nickel and cobalt) catalysts. *Int J Hydrogen Energy.* 41(48):23287–23300
14. Soulé J-F, Miyamura H, Kobayashi S (2011) Powerful amide synthesis from alcohols and amines under aerobic conditions catalyzed by gold or gold/iron,-nickel or-cobalt nanoparticles. *J Am Chem Soc* 133(46):18550–18553
15. Gamboa-Rosales N, Ayastuy J, Iglesias-González A et al (2012) Oxygen-enhanced WGS over ceria-supported Au–Co₃O₄ bimetallic catalysts. *Chem Eng J* 207:49–56
16. Ajaikumar S, Ahlqvist J, Larsson W et al (2011) Oxidation of α -pinene over gold containing bimetallic nanoparticles supported on reducible TiO₂ by deposition-precipitation method. *Appl Catal A* 392(1–2):11–18
17. Tamasauskaite-Tamasiunaite L, Jagminiene A, Balčiūnaite A et al (2013) Electrocatalytic activity of the nanostructured Au–Co catalyst deposited onto titanium towards borohydride oxidation. *Int J Hydrogen Energy* 38(33):14232–14241
18. Zhang H, Dai B, Wang X et al (2013) Non-mercury catalytic acetylene hydrochlorination over bimetallic Au–Co (III)/SAC catalysts for vinyl chloride monomer production. *Green Chem* 15(3):829–836
19. Wu Z, Zhang L, Guan Q et al (2015) Catalytic oxidation of toluene over Au–Co supported on SBA-15. *Mater Res Bull* 70:567–572
20. Santos D, Balčiūnaite A, Tamašauskaitė-Tamašiūnaite L et al (2016) AuCo/TiO₂-NTs anode catalysts for direct borohydride fuel cells. *J Electrochem Soc* 163(14):1553–1557
21. Pillion JE, Thompson ME (1991) Synthesis and polymerization of propargylamine and aminoacetonitrile intercalation compounds. *Chem Mater* 3(5):777–779
22. Sunderhaus JD, Martin SF (2009) Applications of multicomponent reactions to the synthesis of diverse heterocyclic scaffolds. *Chem Eur J* 15(6):1300–1308
23. Maruyama W, Akao Y, Youdim MB et al (2001) Transfection-enforced Bcl-2 overexpression and an anti-Parkinson drug, rasagiline, prevent nuclear accumulation of glyceraldehyde-3-phosphate dehydrogenase induced by an endogenous dopaminergic neurotoxin, N-methyl (R) salsolinol. *J Neurochem* 78(4):727–735
24. de Sousa FT, da Silva MR, de Oliveira MdCF et al (2015) Chemoenzymatic synthesis of rasagiline mesylate using lipases. *Appl Catal, A* 492:76–82
25. Naoi M, Maruyama W, Youdim MBH et al (2003) Anti-apoptotic function of propargylamine inhibitors of type-B monoamine oxidase. *Inflammopharmacology* 11(2):175–181
26. Lo VKY, Kung KKY, Wong MK et al (2009) Gold(III) ((CN)₂-N-Lambda) complex-catalyzed synthesis of propargylamines via a three-component coupling reaction of aldehydes, amines and alkynes. *J Organomet Chem* 694(4):583–591
27. Price GA, Brisdon AK, Flower KR et al (2014) Solvent effects in gold-catalysed A₃-coupling reactions. *Tetrahedron Lett* 55(1):151–154
28. Xiao F, Chen Y, Liu Y et al (2008) Sequential catalytic process: synthesis of quinoline derivatives by AuCl₃/CuBr-catalyzed three-component reaction of aldehydes, amines, and alkynes. *Tetrahedron* 64(12):2755–2761
29. Kung KKY, Li GL, Zou L et al (2012) Gold-mediated bifunctional modification of oligosaccharides via a three-component coupling reaction. *Org Biomol Chem* 10(5):925–930
30. Srinivas V, Koketsu M (2013) Synthesis of indole-2-, 3-, or 5-substituted propargylamines via gold(III)-catalyzed three component reaction of aldehyde, alkyne, and amine in aqueous medium. *Tetrahedron* 69(37):8025–8033
31. Wen-Wen C, Hai-Peng B, Chao-Jun L (2010) The first cobalt-catalyzed transformation of alkynyl C–H bond: aldehyde-alkyne-amine (A³) coupling. *Synlett* 3:475–479
32. Layek S, Agrahari B, Kumari S et al (2018) [Zn(l-proline)₂] catalyzed one-pot synthesis of propargylamines under solvent-free conditions. *Catal Lett* 148(9):2675–2682
33. Shore G, Yoo W-J, Li C-J et al (2009) Propargyl amine synthesis catalysed by gold and copper thin films by using microwave-assisted continuous-flow organic synthesis (MACOS). *Chem Eur J* 16(1):126–133
34. Layek K, Chakravarti R, Kantam ML et al (2011) Nanocrystalline magnesium oxide stabilized gold nanoparticles: an advanced nanotechnology based recyclable heterogeneous catalyst platform for the one-pot synthesis of propargylamines. *Green Chem* 13(10):2878–2887
35. Chng LL, Yang J, Wei Y et al (2009) Semiconductor-gold nanocomposite catalysts for the efficient three-component coupling of aldehyde, amine and alkyne in water. *Adv Synth Catal* 351(17):2887–2896
36. Gonzalez Bejar M, Peters K, Hallett Tapley GL et al (2013) Rapid one-pot propargylamine synthesis by plasmon mediated catalysis with gold nanoparticles on ZnO under ambient conditions. *Chem Commun* 49(17):1732–1734
37. Huang JL, Gray DG, Li CJ (2013) A(3)-Coupling catalyzed by robust Au nanoparticles covalently bonded to HS-functionalized cellulose nanocrystalline films. *Beilstein J Org Chem* 9:1388–1396
38. Ko HM, Kung KKY, Cui JF et al (2013) Bis-cyclometalated gold(III) complexes as efficient catalysts for synthesis of propargylamines and alkylated indoles. *Chem Commun* 49(78):8869–8871
39. Shabbir S, Lee Y, Rhee H (2015) Au(III) catalyst supported on a thermoresponsive hydrogel and its application to the A-3 coupling reaction in water. *J Catal* 322:104–108
40. Anand N, Ramudu P, Reddy KHP et al (2013) Gold nanoparticles immobilized on lipoic acid functionalized SBA-15: synthesis, characterization and catalytic applications. *Appl Catal A* 454:119–126
41. Villaverde G, Corma A, Iglesias M et al (2012) Heterogenized gold complexes: recoverable catalysts for multicomponent reactions of aldehydes, terminal alkynes, and amines. *ACS Catal* 2(3):399–406
42. Borah BJ, Borah SJ, Saikia K et al (2014) Efficient one-pot synthesis of propargylamines catalysed by gold nanocrystals stabilized on montmorillonite. *Catal Sci Technol* 4(11):4001–4009
43. Liu L, Zhang X, Gao J et al (2012) Engineering metal-organic frameworks immobilize gold catalysts for highly efficient one-pot synthesis of propargylamines. *Green Chem* 14(6):1710–1720
44. Karimi B, Gholinejad M, Khorasani M (2012) Highly efficient three-component coupling reaction catalyzed by gold nanoparticles supported on periodic mesoporous organosilica with ionic liquid framework. *Chem Commun* 48(71):8961–8963
45. Zhang X, Corma A (2008) Supported gold(III) catalysts for highly efficient three-component coupling reactions. *Angew Chem Int Ed* 47(23):4358–4361
46. Jose Climent M, Corma A, Iborra S (2012) Homogeneous and heterogeneous catalysts for multicomponent reactions. *RSC Adv* 2(1):16–58
47. Kidwai M, Bansal V, Kumar A et al (2007) The first Au-nanoparticles catalyzed green synthesis of propargylamines via a three-component coupling reaction of aldehyde, alkyne and amine. *Green Chem* 9(7):742–745
48. Abahmane L, Koehler JM, Gross GA (2011) Gold-nanoparticle-catalyzed synthesis of propargylamines: the traditional A(3)-multicomponent reaction performed as a two-step flow process. *Chem Eur J* 17(10):3005–3010

49. Jiang Y, Zhang X, Dai X et al (2017) Microwave-assisted synthesis of ultrafine Au nanoparticles immobilized on MOF-199 in high loading as efficient catalysts for a three-component coupling reaction. *Nano Res* 10(3):876–889
50. Gholinejad M, Zareh F, Najera C (2018) Iron oxide modified with pyridyl-triazole ligand for stabilization of gold nanoparticles: an efficient heterogeneous catalyst for A3 coupling reaction in water. *Appl Organomet Chem* 32(9):e4454
51. Bhatte KD, Sawant DN, Deshmukh KM et al (2011) Nano-size Co_3O_4 as a novel, robust, efficient and recyclable catalyst for A3-coupling reaction of propargylamines. *Catal Commun* 16(1):114–119
52. Safaei-Ghomi J, Nazemzadeh SH (2017) Ionic liquid-attached colloidal silica nanoparticles as a new class of silica nanoparticles for the preparation of propargylamines. *Catal Lett* 147(7):1696–1703
53. Shirole G, Kadnor V, Gaikwad S et al (2016) Iron oxide-supported copper oxide nanoparticles catalyzed synthesis of propargyl amine derivatives via multicomponent approach. *Res Chem Intermed* 42(5):4785–4795
54. Hekmati M (2019) Application of biosynthesized CuO nanoparticles using *Rosa canina* fruit extract as a recyclable and heterogeneous nanocatalyst for alkyne/aldehyde/amine A3 coupling reactions. *Catal Lett* 149(8):2325–2331
55. Berrichi A, Bachir R, Benabdallah M et al (2015) Supported nano gold catalyzed three-component coupling reactions of amines, dichloromethane and terminal alkynes (AHA). *Tetrahedron Lett* 56(11):1302–1306
56. Sharma RK, Sharma S, Gaba G (2014) Silica nanospheres supported diazafluorene iron complex: an efficient and versatile nanocatalyst for the synthesis of propargylamines from terminal alkynes, dihalomethane and amines. *RSC Adv* 4(90):49198–49211
57. Berrichi A, Bachir R, Bedrane S et al (2019) Heterogeneous bimetallic Au–Co nanoparticles as new efficient catalysts for the three-component coupling reactions of amines, alkynes and CH_2Cl_2 . *Res Chem Intermed* 45(6):3481–3495
58. Drăgan N, Crișan M, Răileanu M et al (2014) The effect of Co dopant on TiO_2 structure of sol–gel nanopowders used as photocatalysts. *Ceram Int* 40(8):12273–12284
59. Wang X, Huang Z, Lu L et al (2015) Preparation and catalytic activities of Au/Co bimetallic nanoparticles for hydrogen generation from NaBH_4 solution. *J Nanosci Nanotechnol* 15(4):2770–2776
60. Yu D, Zhang Y (2011) Copper-catalyzed three-component coupling of terminal alkyne, dihalomethane and amine to propargylic amines. *Adv Synth Catal* 353(1):163–169
61. Nador F, Volpe MA, Alonso F et al (2013) Copper nanoparticles supported on silica coated maghemite as versatile, magnetically recoverable and reusable catalyst for alkyne coupling and cycloaddition reactions. *Appl Catal A* 455:39–45
62. Fodor A, Kiss A, Debreczeni N et al (2010) A simple method for the preparation of propargylamines using molecular sieve modified with copper(ii). *Org Biomol Chem* 8(20):4575–4581
63. Gao J, Song QW, He LN et al (2012) Efficient iron(III)-catalyzed three-component coupling reaction of alkynes, CH_2Cl_2 and amines to propargylamines. *Chem Commun* 48(14):2024–2026

Publisher's Note Springer Nature remains neutral with regard to jurisdictional claims in published maps and institutional affiliations.